V1820 Orionis: an RR Lyrae Star With Strong and Irregular Blazhko Effect

Pierre de Ponthière
15 Rue Pré Mathy, Lesve, Profondeville 5170, Belgium;
pierredeponthiere@gmail.com

Franz-Josef (Josch) Hambsch
12 Oude Bleken, Mol, 2400, Belgium; hambsch@telenet.be

Tom Krajci
P.O. Box 1351, Cloudcroft, NM 88317; tom_krajci@tularosa.net

Kenneth Menzies
318A Potter Road, Framingham, MA, 01701

Patrick Wils
Aarschotsebaan 31, Hever B-3191, Belgium; patrickwils@yahoo.com

Abstract   The Blazhko effect in V1820 Orionis and its period were reported for the first time by Wils *et al.* (*MNRAS*, **368**, 1757; 2006) from a data analysis of the Northern Sky Variability Survey. The results of additional V1820 Orionis observations over a time span of four years are presented herein. From the observed light curves, 73 pulsation maxima have been measured. The times of light maxima have been compared to ephemerides to obtain the (O–C) values. The Blazhko period (27.917 ± 0.002 d) has been derived from light curve Fourier analysis and from ANOVA analyses of the (O–C) values and of magnitudes at maximum light (M_{max}). During one Blazhko cycle, a hump in the ascending branch of the light curve was clearly identified and has also created a double maximum in the light curve. The frequency spectrum of the light curve, from a Fourier analysis with PERIOD04, has revealed triplet, quintuplet structures, and a second Blazhko weak modulation (period = 34.72 ±0.01 d). V1820 Orionis can be ranked as a strongly modulated star based on its observed amplitude and phase variations. The amplitude ratio of the largest triplet component to main pulsation component is quite large: 0.34.

1. Introduction

The star V1820 Orionis is classified in the *General Catalogue of Variable Stars* (Samus *et al.* 2011) as an RR Lyr (RRab) variable star with a period of 0.479067 day and with maximum and minimum V-band magnitudes of 12.5 and 13.4, respectively. This star was identified as an RRab with a Blazhko period of 28 days by Wils *et al.* (2006). At this time the star was classified as NSV 02724

in the *New Catalogue of Suspected Variable Stars* (Kukarkin *et al.* 2011).

The current data were gathered during 157 nights between December 2006 and March 2012. During this period of 1,918 days, a total of 22,592 magnitude measurements covering 70 Blazhko cycles were collected. The 7,300 observations from December 2006 to February 2010 were made by Hambsch using 30-cm and 50-cm telescopes located in Cloudcroft (New Mexico). From September 2011 to March 2012 the observations were made by Hambsch using the telescope in Cloudcroft and a 40-cm telescope in San Pedro de Atacama (Chile). de Ponthière contributed additional measurements with a 20-cm telescope located at Lesve (Belgium).

The comparison stars used by the authors are given in Table 1. The star coordinates and magnitudes in B and V bands were obtained from the NOMAD catalogue (Zacharias *et al.* 2011). C1 was used as a magnitude reference and C2 as a check star. The Johnson V magnitudes from different instruments have not been transformed to the standard system since measurements were performed with only a V filter. However, two simultaneous measurements from the instruments in Cloudcroft and San Pedro de Atacama were observed to differ by only 0.025 mag. Dark and flat field corrections were performed with the MAXIMDL software (Diffraction Limited 2004), aperture photometry was performed using LESVEPHOTOMETRY (de Ponthière 2010) custom software which also evaluates the SNR and estimates magnitude errors.

2. Light curve maxima analysis

The times of maxima of the light curves have been evaluated with custom software (de Ponthiere 2010) fitting the light curve with a smoothing spline function (Reinsch 1967). Table 2 provides the list of observed maxima and Figure 1 shows the (O–C) values.

A linear regression of all available (O–C) values has provided a pulsation period of 0.4790486 d (2.087471 d^{-1}). The (O–C) values have been re-evaluated with this new pulsation period. The new pulsation elements derived from a linear least-square fitting are:

$$\text{HJD}_{\text{Pulsation}} = (2\ 454\ 075.8935 \pm 0.0060) + (0.4790486 \pm 0.0000018)\ \text{E} \quad (1)$$

The folded light curve on this pulsation period is shown in Figure 2.

The Blazhko period was determined by a period analysis of the (O–C) values and the M_{max} (Magnitude at Maximum) values with the ANOVA algorithm of PERANSO (Vanmunster 2007). Both periodograms, presented in Figure 3a and 3b, show a primary peak and a series of aliases equally spaced around the main modulation frequency. The lists of prominent peaks are indicated below.

From (O–C) analysis, the main frequencies and periods are tabulated below:

	Frequency (cycles / day)	Period (days)	Peak value
f_0	0.03637 ± 0.00004	27.50 ± 0.03d	31.8
f_1	0.03583	27.91	27.3
f_2	0.03471	28.81	28.0
f_3	0.03691	27.09	18.2
f_4	0.03747	26.69	20.0

From M_{max} analysis, the main frequencies and periods are tabulated below:

	Frequency (cycles / day)	Period (days)	Peak value
f_0	0.03581 ± 0.00004	27.92 ± 0.03d	154.1
f_1	0.03527	28.35	69.6
f_2	0.03471	28.81	61.7
f_3	0.03637	27.50	63.2
f_4	0.03693	27.08	36.3

These aliases are apparently due to the presence of two groups of measurements separated by four years. The first group of 13 maxima is centered on January 2007 and the second group of 52 maxima is centered on December 2011. The alias spacing of 0.00054 d^{-1} (1,851 d) is approximately the reciprocal of the time span between the two measurement groups (that is, 59 months or 1,770 days). A Spectral Window analysis on (O–C) and M_{max} data points provided peaks separated by 0.00057 d^{-1} (1754d), which supports the origin of the aliases.

From the (O–C) period analysis it is not possible to deduce which peak corresponds to the Blazhko period since none of them is emerging significantly. However, the prominent peak of the M_{max} analysis is also found as an important peak in the (O–C) analysis. Therefore, the Blazhko period is estimated as 27.92 $\pm$ 0.03 days. Wils *et al.* (2006) have reported a value of 28 days.

The highest recorded maximum was observed at HJD 2455955.6847, and the Blazhko ephemeris origin has been selected as 69 Blazhko cycles before this highest recorded maximum. On the basis of this origin, the first observations have a positive value for $E_{Blazhko}$.

$$HJD_{Blazhko} = 2454029.2047 + (27.92 \pm 0.03) \, E_{Blazhko} \qquad (2)$$

The folded (O–C) and M_{max} versus the Blazhko phase curves are presented in Figures 4 and 5. The magnitudes at maximum values differ by about 0.85 magnitude, that is, 52% of the light curve peak to peak variations. If the humps are not taken into account, the (O–C) values differ in a range of 0.075 day, that is, 15% of the pulsation period.

RR Lyrae stars of type RRab are known to frequently show a hump in their light curves that appears before light maximum (Smith 1995). The evolution of a strong hump during five consecutive nights (JD 2455941 to 2455945) was observed. The folded light curves for those nights (JD41–45) are given in Figure 6. During the first night (JD 2455941), the shape of the maximum appears normal, but on the second night (JD 2455942) the light curve shows a shoulder in the decreasing branch. On JD 2455943 two maxima are separated by 0.0685 day (that is, 14% of the pulsation period) and on the fourth night, the maximum is preceded by a classical hump in the increasing branch. The (O–C) values for the maxima occurring on nights JD 2455941, JD 2455942, and for the first maximum on night JD 2455943 appear to be outliers in the (O–C) diagram (Figure 1), but the (O–C) value of the shoulder on the second night JD 2455942 is close to what is expected. The evolution of a shockwave phenomenon generating the hump has probably distorted the light curve on JD 2455942 to the point that the magnitude of the hump is larger than at normal maximum magnitude. The same phenomenon is not repeated at each Blazhko cycle, but it probably occurred on nights of JD 2454126 and JD 2454770 as the corresponding (O–C) values appear to be outliers in the (O–C) diagram (Figure 1). These irregularities in the (O–C) values occur around the Blazhko phase equal to 0.5 (Figure 4). The observed shoulder in the decreasing branch on JD 2455942 is similar to the "bump" detected by Jurcsik *et al.* (2012) in the RZ Lyrae light curve. This phenomenon of light curve distortion for both stars occurs when the Blazhko amplitude modulation is weakest. The bump appearing in the descending branch of RZ Lyrae occurs around pulsation phase 0.25–0.30 but the shoulder in the decreasing branch of V1820 Orionis happens around pulsation phase 0.0. Based on the different pulsation phases at which the light curve distortions occur and the night-to-night evolution for V1820 Orionis, it can be supposed that the phenomena are probably different for the two stars.

The relationship between M_{max} and (O–C) can be plotted on a diagram. These two quantities vary with the Blazhko phase and if they are repetitive from cycle to cycle, the data will lie on a loop and if they are sinusoidal the loop will be elliptical. The loop will run in a clockwise progression if the M_{max} has positive phase delay versus (O–C) phase and vice-versa. However M_{max} and (O–C) values for V1820 Orionis, represented by small diamonds in Figure 7, are poorly repetitive from cycle to cycle and are largely scattered. The mean values of (O–C) and M_{max} have been evaluated for 10 bins of the Blazhko phase and are represented as large squares in the Figure 7. An inspection of the successive points indicates that the loop is progressing in counter-clockwise direction. The point in the lower left of the diagram with (O–C = –0.1 day) corresponds to the strong hump described above. Le Borgne *et al.* (2012) have shown that for most of the analyzed Blazhko stars the M_{max} versus (O–C) diagrams exhibit a similar counterclockwise rotation.

3. Frequency spectrum analysis

A Blazhko effect on the light curve can be modeled as an amplitude and/or phase modulation of the periodic pulsation, with the reciprocal of the modulation frequency being the Blazhko period. Szeidl and Jurcsik (2009) have shown that the Fourier spectrum of an amplitude and phase modulation model is given by an infinite series including the fundamental frequency (f_0), harmonic frequencies (if_0), and multiplet frequencies ($if_0 \pm jf_B$).

$$m(t) = \Sigma\, A_i \sin(i\omega t + \Phi_{i0}) + \Sigma\Sigma\, A^+_{ij} \sin[(i\omega + j\Omega)t + \Phi^+_{ij}]$$
$$+ \Sigma\Sigma\, A^-_{ij} \sin[(i\omega - j\Omega)t + \Phi^-_{ij}] \tag{3}$$

where:

$\omega = 2\pi f_0$, f_0 is the fundamental frequency of the light-curve,
$\Omega = 2\pi f_B$, f_B is the Blazhko modulation frequency, and
A_i A^+_{ij} A^-_{ij} are the Fourier coefficients and Φ_i, Φ^+_{ij} and Φ^-_{ijj} their phase angles, "i" indices are used for the fundamental and the harmonic frequencies and "j" indices for the side lobes (for example, A^+_{32} is the coefficient of the multiplet ($3f_0 + 2f_B$) .

The methodology used herein is similar to the one reported by Kolenberg (2009) where triplet and quintuplet components were detected in the spectrum of SS Fornacis. The spectral analysis was performed with PERIOD04 (Lenz and Breger 2005) to yield a Fourier analysis and multi-frequency sine-wave fitting.

The sine-wave fitting was determined by successive data pre-whitening and Fourier analysis on residuals. For each observed harmonic and triplet, the signal-to-noise ratio has been evaluated to retain only significant signals, that is, with an SNR greater than 3.5. During the PERIOD04 sine-wave fitting process, only the fundamental f_0 and the first main triplet component $f_0 + f_B$ frequencies have been unconstrained; the other frequencies have been entered as combinations of f_0 and $f_0 + f_B$. Table 3 provides the amplitude and phase for each Fourier component obtained with the best sine-wave fitting. The uncertainties of frequencies, amplitudes, and phases have been estimated by Monte Carlo simulations. As it is known that Monte Carlo simulation uncertainties can be underestimated (Kolenberg *et al.* 2009), the uncertainty values have been multiplied by a factor of two. The harmonics of f_0 are significant to the eighth order. The residuals after subtraction of the best fit based on f_0 and harmonics up to the eighth order is provided in Figure 8a. The large residuals close to the phase of maximum light (0.8 to 1.1) are due to amplitude and phase modulations created by the Blazhko effect. The residuals are reduced significantly when the side peaks (triplets) around the f_0 frequency and harmonics up to the seventh order are included in the fitting process (Figure 8b).

The fundamental pulsation frequency f_0 (2.08747 d^{-1}) is very close to the frequency obtained from a linear regression analysis of time of maxima. The

Blazhko period was also measured from the first side peak frequency $f_0 + f_B$ and f_0 to yield $f_B = (2.12329 - 2.08747) = 0.03582$ d^{-1} and $P_B = 27.917 \pm 0.002$ days. The second side peak frequency $f_0 - f_B$ exhibited a lower amplitude and higher uncertainty and was not used for Blazhko period evaluation. The Blazhko period found with the sine-wave fitting method (27.919 ± 0.002 days) is equal to the value found with the brightness at maximum analysis (27.92 ± 0.03 days). Table 4 lists the harmonic and significant amplitude ratios. One useful parameter to quantify the Blazhko effect is the amplitude ratio $A^{\pm}_{11} / A_1$, where $A^{\pm}_{11}$ is the amplitude of the largest side lobe at $f_0 + f_B$ or $f_0 - f_B$ and A_1 is the amplitude of f_0. The most common and maximum values for this ratio are 0.15 and 0.4, respectively (Alcock *et al.* 2003). With an amplitude ratio $A_{11}^{+} / A_1 = 0.34$, V1820 Orionis can be ranked as strongly modulated.

The triplet ratios $R_i = A^+_{i1} / A^-_{i1}$ and asymmetries $Q_i = (A^+_{i1} - A^-_{i1}) / (A^+_{i1} + A^-_{i1})$ are also provided in Table 4. The asymmetry in the side lobes observed for V1820 Orionis is not unexpected on the basis of Szeidl and Jurcsik (2009), which showed that this asymmetry is related to the phase difference between the Blazhko amplitude and phase modulations. If the Blazhko effect were limited to amplitude modulation, the ratios R_i and Q_i would be equal to 1 and 0, respectively. The asymmetry ratios Q_i around 0.35 are a sign that V1820 Orionis is amplitude- and phase-modulated.

Besides the harmonics and triplets, some quintuplet components ($kf_0 + 2f_B$) and a peak at the Blazhko period itself were found. And finally, two modulation peaks appear in the spectrum around f_0 and $2f_0$ with a separation of 0.028 d^{-1}. They correspond to a second Blazhko modulation f_{B2} ($1/f_{B2} = 34.72 \pm 0.01$ days). This phenomenon of multi-periodic modulation has also been detected by Sódor *et al.* (2011) in the spectrum of CZ Lacertae. In the case of CZ Lac, the modulation components of the two frequencies (f_B and f_{B2}) have similar amplitudes, which is not the case for V1820 Orionis. The second modulation frequency f_{B2} has weaker components than f_B, but they remain significant as their SNR are 9.2 and 6.0, respectively. A spectral analysis on M_{max} values provides the same two Blazhko modulation frequencies f_B and f_{B2}, which are in a 5:4 resonance ratio. The corresponding beating period is 139 days, which is visible on the multi-frequency sine-wave fitting obtained with PERIOD04 (Figure 9). For clarity, Figure 9 only includes the last observation season (2011–2012). A 5:4 resonance ratio was also found between the two modulation frequencies of CZ Lac during the 2004 observation season (Sódor *et al.* 2011) but the next year this resonance ratio changed to a value of 4:3.

4. Light curve variations over Blazhko cycle

In order to investigate the light curve variations over the Blazhko cycle, the complete dataset was subdivided into ten temporal subsets corresponding to different Blazhko phase intervals Ψ_i ($i = 0,9$). The ephemeris derived previously

during the analysis of light curve maxima was used to define the epoch of the Blazhko zero phase (HJD = 2454029.2047). The data points are relatively well distributed over the subsets with the number of data points in each subset varying between 1,144 and 3,045. The light curves for each subset are presented in Figure 10. The strong hump observed during JD 2455942, as described previously, is highlighted in red in the panel of subset ($\Psi = 0.5$–0.6).

For each subset, the amplitude A_i and phase Φ_i of of the fundamental and harmonic frequencies up to the fourth order have been evaluated with the Least-Square Fit module of PERIOD04. The amplitudes and epoch-independent phase differences ($\Phi_{k1} = \Phi_k - k\Phi_1$) over the Blazhko cycle are provided in Table 4 and exhibited in Figures 11a and 11b. As expected, the amplitude of the fundamental frequency is clearly lower at a Blazhko phase around 0.5, that is, when the light curve amplitude variation on the pulsation cycle is weaker. The maximum and minimum Φ_1 phase values (2.234 and 1.253 radians) are found in subsets Ψ (0.4–0.5) and Ψ (0.1–0.2), respectively. The difference between maximum and minimum Φ_1 phase is a measure of the phase modulation strength and is equal to $(2.234 - 1.253) = 0.981$ radian or 0.156 cycle, which corresponds roughly to the value of 15 % noted for the peak to peak deviation of (O–C). The phase variation of harmonic component Φ_{41} is the largest, with a value of 3.6 radians, while Φ_{21} varies only by 0.37 radians over the Blazhko cycle. The phase variation of harmonic component Φ_{41} is very large as compared to Φ_{k1} values of 1 and 0.5 radians observed for RZ Lyrae (Jurcsik *et al.* 2012) and SS Fornacis (Kolenberg *et al.* 2009), respectively.

Figure 12 provides a graph of the A_1 coefficient versus the Φ_1 for the different subsets. This graph is similar to the graph of the Magnitude at Maximum versus (O–C) given in Figure 7. In order to compare the two graphs, the Φ_1 axis of Figure 12 was inverted. Indeed, for the sine-wave fitting $[A_i \sin(\omega_i t + \Phi_i)]$, a larger Φ_i phase corresponds to a time advance, that is, a lower value of (O–C). With the Φ_1 axis inverted, the loop of A_1 values exhibits a counter-clockwise progression as in Figure 7.

5. Conclusions

The strong and irregular Blazhko behavior of V1820 Ori has been exhibited by two different methods: (1) measurement of light curve maxima, and (2) Fourier analysis. The latter method, Fourier analysis, has been feasible due to the large number of regular observations over the pulsation period which was not limited to the times of light curve maxima. Both methods yield the same results for the fundamental pulsation period (0.4790486 day ± 0.0000018) and the Blazhko period (27.917 days ± 0.002). The irregularities of the Blazhko effect are probably explained by variations of the strength of a shockwave phenomenon generating the hump in the ascending branch of the light curve. This erratic behavior generally occurs around a Blazhko phase of 0.5. Measured

ratios of Fourier amplitudes and their asymmetries also confirm strong Blazhko amplitude and phase modulations. A second weaker Blazhko modulation with a period 34.70 ±0.02 days has also been identified. The two modulation frequencies are in a 5:4 resonance ratio.

6. Acknowledgements

References

Alcock, C., *et al.* 2003, *Astrophys. J.*, **598**, 597.

de Ponthière, P. 2010, Lesvephotometry, automatic photometry software (http://www.dppobservatory.net).

Diffraction Limited. 2004, maximdl image processing software (http://www.cyanogen.com).

Jurcsik, J., *et al.* 2012, *Mon. Not. Roy. Astron. Soc.*, **423**, 993.

Kolenberg, K., *et al.* 2009, *Mon. Not. Roy. Astron. Soc.*, **396**, 263.

Kukarkin, B., *et al.* 2011, *New Catalogue of Suspected Variable Sars* (NSV database, Version 2011 March, http://www.sai.msu.su/gcvs/gcvs/nsv/nsv.dat).

Le Borgne, J. F., *et al.* 2012, *Astron. J.*, **144**, 39.

Lenz, P., and Breger, M. 2005, *Commun. Asteroseismology*, **146**, 53.

Reinsch, C. H. 1967, *Numer. Math.*, **10**, 177.

Samus, N. N., *et al.* 2011 *General Catalogue of Variable Stars* (GCVS database, Version 2011 January, http://www.sai.msu.su/gcvs/gcvs/index.htm).

Smith, H. 1995, *RR Lyrae Stars*, Cambridge Univ. Press, Cambridge.

Sódor, Á., *et al.* 2011, *Mon. Not. Roy. Astron. Soc.*, **411**, 1585.

Szeidl, B., and Jurcsik, J. 2009 *Commun. Asteroseismology*, **160**, 17.

Vanmunster, T. 2007, peranso, period analysis software (http://www.cbabelgium.com and http://www.peranso.com).

Wils, P., Lloyd, C., and Bernhard, K. 2006, *Mon. Not. Roy. Astron. Soc.*, **368**, 1757.

Zacharias, N., Monet, D., Levine, S., Urban, S., Gaume, R., and Wycoff, G. 2011, The Naval Observatory Merged Astrometric Dataset (NOMAD, http://www.usno.navy.mil/USNO/astrometry/optical-IR-prod/nomad/).

Table 1. Comparison stars for V1820 Ori.

Identification	R. A. (2000)			Dec. (2000)			B	V	B-V	
	h	m	s	°	′	″				
GSC 125-41	05	54	57.4	+04	56	42.5	13.83	13.31	0.52	C1
GSC 125-341	05	54	29.6	+04	53	59.1	14.94	13.65	1.29	C2

Table 2. List of measured maxima of V1820 Ori.

Maximum HJD	Error	O–C (day)	E	VMagnitude	Error	Filter	Location[a]	Remark[b]
2454075.9173	0.0033	0.0235	0	12.367	0.007	C	1	
2454076.8783	0.0035	0.0264	2	12.330	0.006	C	1	
2454079.7429	0.0020	0.0167	8	12.083	0.005	C	1	
2454085.9515	0.0011	–0.0024	21	11.851	0.005	C	1	
2454104.6673	0.0028	0.0306	60	12.342	0.005	C	1	
2454110.8696	0.0007	0.0053	73	11.902	0.004	C	1	
2454114.6902	0.0008	–0.0065	81	11.844	0.003	C	1	
2454126.6093	0.0023	–0.0636	106	12.393	0.004	C	1	*
2454135.7878	0.0015	0.0130	125	12.158	0.004	C	1	
2454136.7440	0.0018	0.0111	127	12.122	0.004	C	1	
2454137.6982	0.0009	0.0072	129	12.021	0.003	C	1	
2454149.6405	0.0012	–0.0267	154	12.118	0.004	C	1	
2454162.6332	0.0023	0.0317	181	12.299	0.004	C	1	
2454439.9682	0.0039	–0.00205	760	12.348	0.005	V	1	
2454748.9571	0.0035	0.00096	1405	12.132	0.007	V	1	
2454749.9218	0.0053	0.00757	1407	12.046	0.043	V	1	
2454770.8990	0.0036	–0.09334	1451	12.370	0.021	C	1	*
2454832.7977	0.0025	0.00818	1580	12.288	0.009	V	1	
2455245.7039	0.0019	–0.02490	2442	12.356	0.011	V	1	
2455813.8853	0.0011	0.00570	3628	11.827	0.008	V	2	
2455824.8744	0.0027	–0.02330	3651	12.203	0.010	V	2	
2455825.8249	0.0034	–0.03090	3653	12.242	0.009	V	2	
2455845.9745	0.0025	–0.00131	3695	11.798	0.016	V	2	
2455859.8570	0.0033	–0.01120	3724	12.428	0.009	V	2	
2455861.7776	0.0045	–0.00679	3728	12.444	0.009	V	2	
2455871.8475	0.0023	0.00310	3749	11.870	0.017	V	2	
2455872.8024	0.0017	–0.00009	3751	11.886	0.008	V	2	
2455873.7629	0.0018	0.00231	3753	11.923	0.010	V	2	
2455881.8771	0.0048	–0.02730	3770	12.225	0.018	V	2	
2455883.8157	0.0026	–0.00490	3774	12.281	0.010	V	2	
2455884.7742	0.0037	–0.00449	3776	12.288	0.010	V	2	
2455885.7271	0.0035	–0.00969	3778	12.298	0.009	V	2	
2455886.6856	0.0027	–0.00928	3780	12.325	0.009	V	2	
2455887.6455	0.0032	–0.00748	3782	12.326	0.009	V	2	

Table 2. List of measured maxima of V1820 Ori, cont.

Maximum HJD	Error	O–C (day)	E	VMagnitude	Error	Filter	Location[a]	Remark[b]
2455894.8573	0.0022	0.01860	3797	12.137	0.010	V	2	
2455895.8119	0.0023	0.01511	3799	12.080	0.010	V	2	
2455896.7562	0.0016	0.00131	3801	11.981	0.020	V	2	
2455896.7649	0.0020	0.01001	3801	11.924	0.009	V	2	
2455897.7287	0.0028	0.01572	3803	11.998	0.009	V	2	
2455898.6824	0.0016	0.01132	3805	11.955	0.009	V	2	
2455899.6376	0.0015	0.00842	3807	11.970	0.010	V	2	
2455900.5927	0.0028	0.00543	3809	11.977	0.014	V	2	
2455905.8498	0.0051	–0.00700	3820	12.129	0.026	V	2	
2455906.8131	0.0045	–0.00179	3822	12.171	0.032	V	2	
2455907.7555	0.0041	–0.01749	3824	12.189	0.027	V	2	
2455908.7226	0.0060	–0.00849	3826	12.269	0.032	V	2	
2455909.6812	0.0063	–0.00798	3828	12.373	0.014	V	2	
2455910.6170	0.0051	–0.03028	3830	12.339	0.012	V	2	
2455919.7662	0.0033	0.01701	3849	12.220	0.014	V	2	
2455930.7657	0.0041	–0.00159	3872	11.928	0.023	V	1	
2455931.7210	0.0024	–0.00438	3874	11.965	0.025	V	1	
2455932.6809	0.0024	–0.00258	3876	12.074	0.019	V	1	
2455941.7342	0.0050	–0.05119	3895	12.461	0.010	V	2	*
2455942.6755	0.0028	–0.06799	3897	12.399	0.009	V	2	*
2455943.6482	0.0064	–0.05338	3899	12.502	0.010	V	2	*
2455943.7167	0.0074	0.01512	3899	12.533	0.010	V	2	
2455944.6666	0.0084	0.00692	3901	12.514	0.009	V	2	
2455945.6294	0.0025	0.01163	3903	12.466	0.016	V	1	
2455945.6433	0.0072	0.02553	3903	12.446	0.009	V	2	
2455946.6153	0.0072	0.03943	3905	12.442	0.018	V	1	
2455946.6215	0.0066	0.04563	3905	12.411	0.009	V	2	
2455947.5790	0.0064	0.04504	3907	12.347	0.010	V	2	
2455948.5257	0.0031	0.03364	3909	12.228	0.010	V	2	
2455953.7740	0.0017	0.01241	3920	11.822	0.015	V	1	
2455954.2495	0.0026	0.00886	3921	11.838	0.015	V	3	
2455955.6847	0.0015	0.00692	3924	11.681	0.014	V	2	
2455956.6423	0.0012	0.00643	3926	11.734	0.013	V	1	
2455957.5987	0.0013	0.00473	3928	11.729	0.020	V	1	
2455964.2835	0.0037	–0.01714	3942	12.284	0.014	V	3	
2455978.6990	0.0030	0.02692	3972	12.177	0.009	V	1	
2455979.6582	0.0022	0.02803	3974	12.066	0.009	V	1	
2455980.6063	0.0012	0.01803	3976	11.953	0.009	V	1	
2455989.6865	0.0029	–0.00368	3995	12.018	0.020	V	1	

[a]Locations: 1—Cloudcroft; 2—Chile; 3—Lesve. [b]Remarks: *—hump

Table 3. Multi–frequency fit results for V1820 Ori. The frequency uncertainties on f_0, $f_0 + f_B$, and $f_0 + f_{B2}$ are 4×10^{-7}, 2×10^{-6}, and 7×10^{-6}, respectively. The values displayed in italics correspond to components not exceeding a SNR greater than 3.5.

Parameter	$f\,(d^{-1})$	$A_i\,(mag)$	$\Phi(cycle)$	$\sigma(\Phi)$	SNR
f_0	2.087466	0.335	0.245768	0.001	82.1
$2f_0$	4.174932	0.126	0.851262	0.002	34.8
$3f_0$	6.262398	0.062	0.459455	0.003	19.8
$4f_0$	8.349864	0.031	0.070836	0.006	11.6
$5f_0$	10.43733	0.020	0.703054	0.010	8.3
$6f_0$	12.5248	0.014	0.296387	0.014	6.1
$7f_0$	14.61226	0.011	0.914742	0.016	5.4
$8f_0$	16.69973	0.007	0.506391	0.028	3.3
f_B	0.035824	0.026	0.113932	0.007	5.8
$f_0 + f_B$	2.12329	0.114	0.08408	0.002	28.0
$f_0 - f_B$	2.051642	0.056	0.16969	0.003	13.8
$2f_0 + f_B$	4.210756	0.078	0.672295	0.003	21.8
$2f_0 - f_B$	4.139108	0.040	0.756026	0.005	11.2
$3f_0 + f_B$	6.298222	0.065	0.335476	0.003	20.7
$3f_0 - f_B$	6.226574	0.032	0.435456	0.006	10.2
$4f_0 + f_B$	8.385687	0.041	0.972183	0.005	15.4
$4f_0 - f_B$	8.31404	0.019	0.089832	0.010	7.2
$5f_0 + f_B$	10.47315	0.024	0.599442	0.008	9.9
$5f_0 - f_B$	10.40151	0.011	0.722088	0.017	4.8
$6f_0 + f_B$	12.56062	0.016	0.183182	0.012	7.1
$6f_0 - f_B$	12.48897	0.007	0.299414	0.027	3.2
$7f_0 + f_B$	14.64809	0.012	0.783367	0.016	5.6
$f_0 + 2f_B$	2.159114	0.014	0.494921	0.015	3.3
$3f_0 + 2f_B$	6.334046	0.021	0.081559	0.009	6.7
$4f_0 + 2f_B$	8.421511	0.023	0.818861	0.009	8.5
$f_0 + f_{B2}$	2.116266	0.028	0.90776	0.007	7.0
$2f_0 + f_{B2}$	4.203732	0.024	0.509457	0.008	6.7

Table 4. V1820 Ori Harmonic, Triplet amplitudes, ratios, and asymmetry parameters.

k	A_i/A_1	A_{i1}^+/A_1	A_{i1}^-/A_1	R_i	Q_i
1	1.00	0.34	0.17	2.01	0.34
2	0.37	0.23	0.12	1.96	0.32
3	0.18	0.19	0.10	2.02	0.34
4	0.09	0.12	0.06	2.14	0.36
5	0.06	0.07	0.03	2.08	0.35
6	0.04	0.05	0.02	2.20	0.37
7	0.03	—	—	—	—
8	0.02	—	—	—	—

Table 5. V1820 Ori. Fourier coefficients over Blazhko cycle.

Ψ (cycle)	A_1 (mag.)	A_2 (mag.)	A_3 (mag.)	A_4 (mag.)	Φ_1 (rad.)	Φ_{21} (rad.)	Φ_{31} (rad.)	Φ_{41} (rad.)
0.0–0.1	0.466	0.223	0.149	0.108	1.411	2.225	4.642	0.873
0.1–0.2	0.432	0.188	0.134	0.070	1.253	2.134	4.667	0.910
0.2–0.3	0.367	0.156	0.100	0.039	1.368	2.219	4.604	0.814
0.3–0.4	0.320	0.150	0.080	0.032	1.752	2.269	4.897	1.293
0.4–0.5	0.240	0.100	0.028	0.016	2.234	2.180	5.353	2.206
0.5–0.6	0.219	0.094	0.042	0.016	2.227	2.323	5.948	4.482
0.6–0.7	0.231	0.055	0.018	0.016	1.567	2.485	5.091	2.699
0.7–0.8	0.326	0.112	0.047	0.014	1.344	2.503	5.267	2.544
0.8–0.9	0.401	0.172	0.098	0.055	1.266	2.269	4.809	1.052
0.9–1.0	0.462	0.211	0.149	0.099	1.275	2.362	4.777	1.051
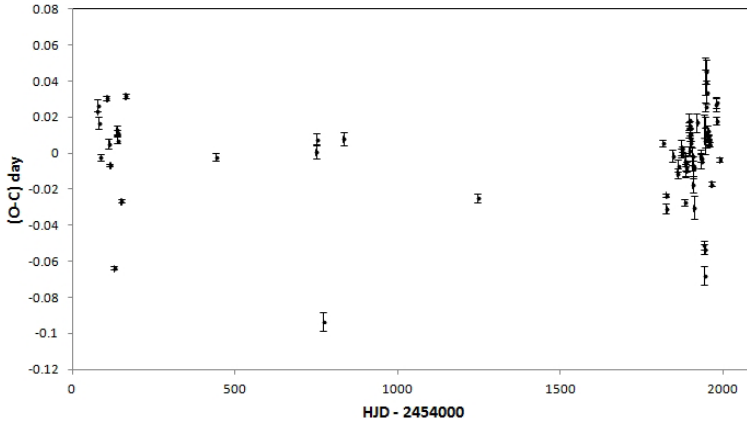
Figure 1. V1820 Ori (O–C).
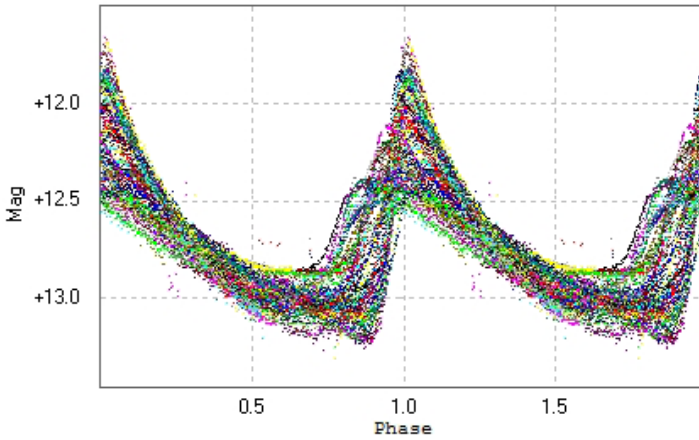
Figure 2. V1820 Ori light curve folded with pulsation period.
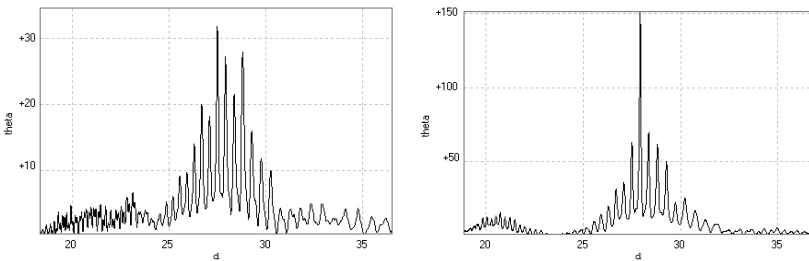
Figure 3a (left). V1820 Ori (O–C) periodogram. Figure 3b (right). V1820 Ori magnitude at maximum periodogram.
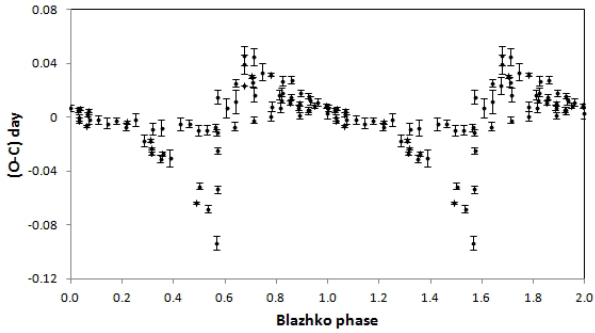
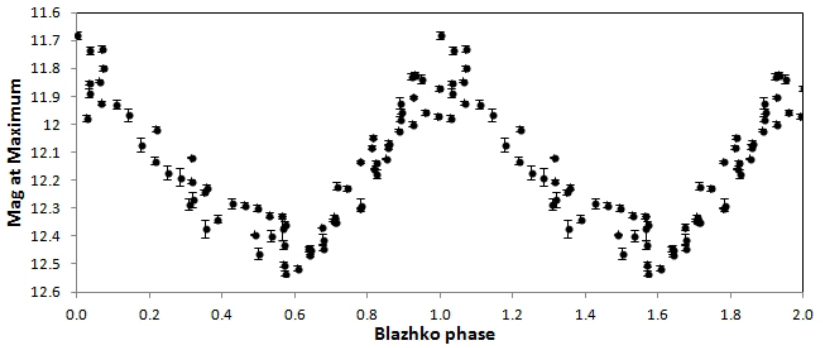Figure 4. V1820 Ori O–C (days) versus Blazhko phase.

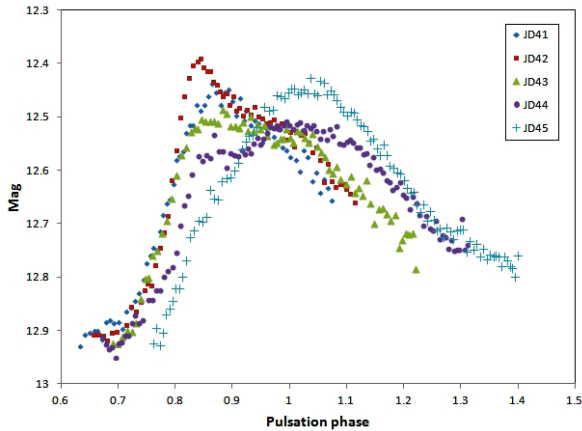Figure 5. V1820 Ori magnitude at maximum versus Blazhko phase.

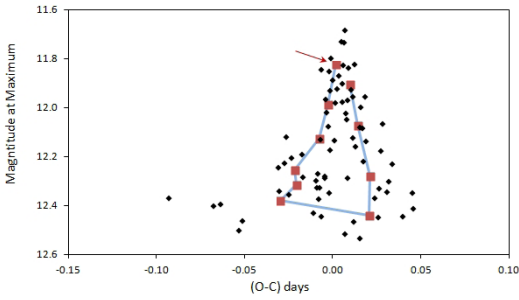Figure 6. V1820 Ori hump evolution for nights JD 2455941 to 2455945.

Figure 7. V1820 Ori magnitude at maximum versus O–C (days) values. Individual values and their means are represented as small diamonds and large squares, respectively. The point corresponding to the bin nearest to 0.0 Blazhko phase is indicated by an arrow.
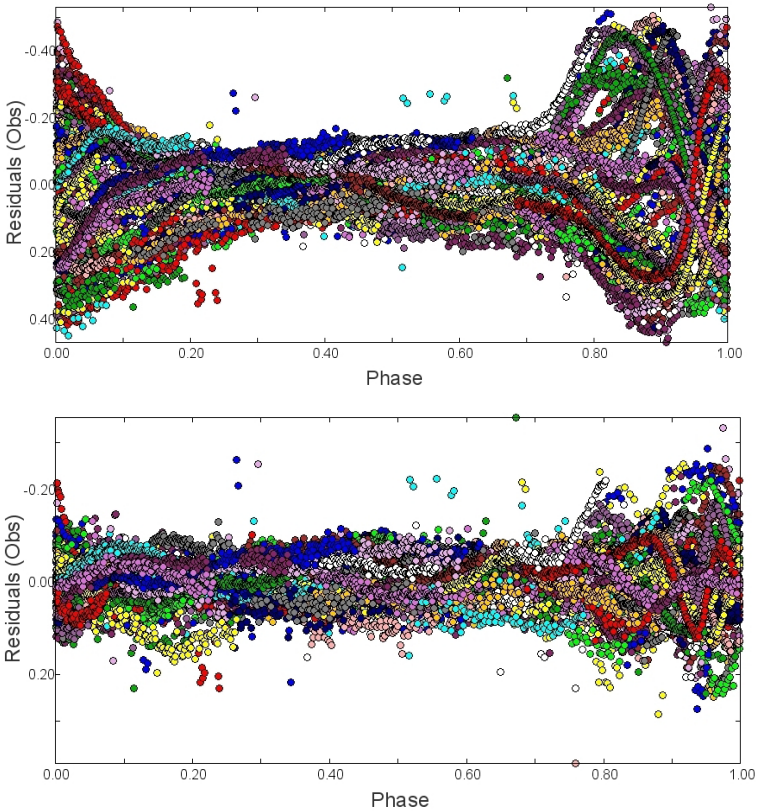
Figure 8a (top). V1820 Ori, residuals after harmonics whitening. Figure 8b (bottom). V1820 Ori residuals after triplet whitening.
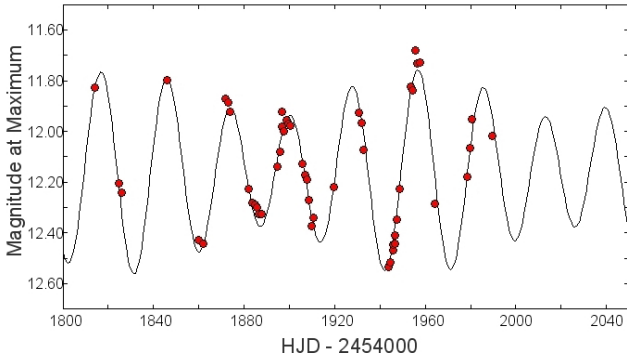
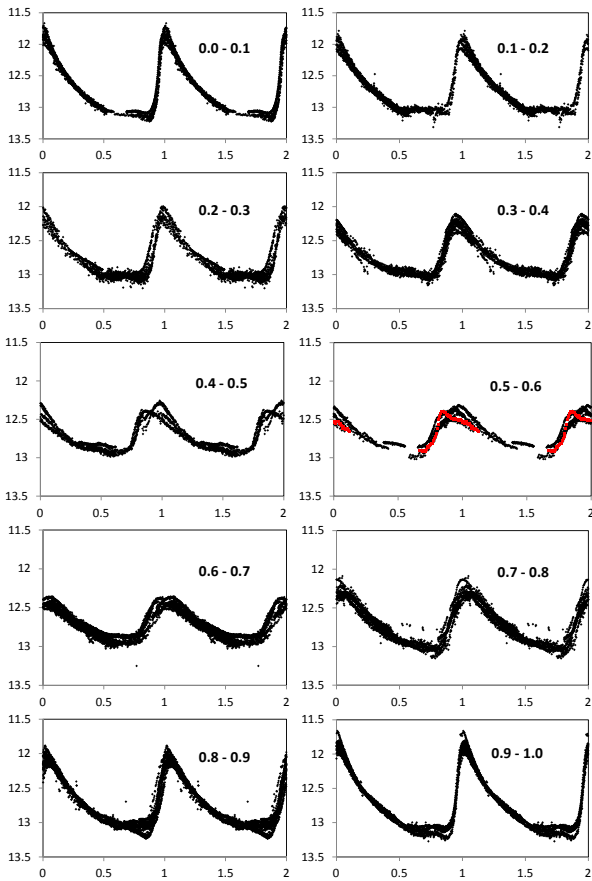Figure 9. V1820 Ori magnitude at maximum curve fitting.

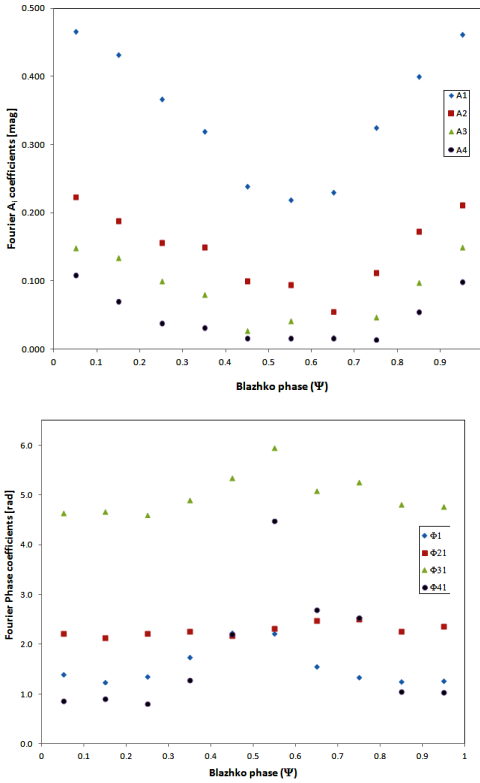Figure 10. V1820 Ori light curve for different Blazhko subsets.

Figure 11a (top). V1820 Ori Fourier A_i amplitude (magnitude) variations versus Blazhko Ψ_i subsets. Figure 11b (bottom). V1820 Ori Fourier Φ_1 and Φ_{k1} phase (rad.) variations versus Blazhko Ψ_i subsets.
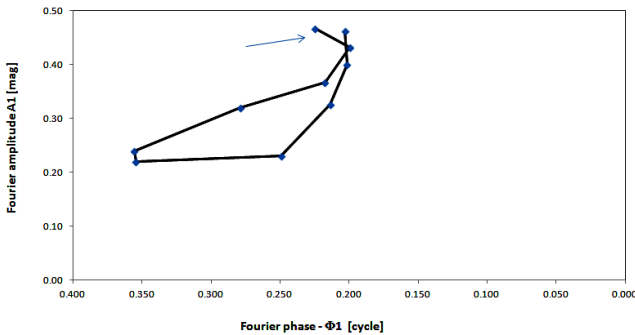

Figure 12. V1820 Ori Fourier amplitude A_1 versus phase Φ_1 for different Blazhko subsets. The point corresponding to the bin nearest to 0.0 Blazhko phase is indicated by an arrow.